

Review

Fatigue Properties of Ti Alloys with an Ultrafine Grained Structure: Challenges and Achievements

Irina Petrovna Semenova ^{1,*}, Yulia Mikhailovna Modina ¹, Andrey Gennadievich Stotskiy ¹,
Alexander Vadimovich Polyakov ^{1,2} and Mikhail Vladimirovich Pesin ²

¹ Institute of Physics of Advanced Materials, Ufa State Aviation Technical University, 12 K. Marx Str., 450008 Ufa, Russia; modina_yulia@mail.ru (Y.M.M.); stockii_andrei@mail.ru (A.G.S.); alex-v.polyakov@mail.ru (A.V.P.)

² Mechanical Engineering Faculty, Perm National Research Polytechnic University, 29 Komsomolsky Pr., 614990 Perm, Russia; m.pesin@mail.ru

* Correspondence: semenova-ip@mail.ru

Abstract: Ultrafine-grained (UFG) structure formation in Ti alloys, by severe plastic deformation (SPD) processing and enhancement of their mechanical properties, including fatigue properties, has been demonstrated in numerous studies in the past 20 years. The present overview analyzes the fatigue properties achieved to date in Ti alloys subjected to SPD. Such aspects are examined as the effect of a UFG structure on the fatigue behavior of commercially pure (CP) Ti, two-phase Ti alloys, using the popular Ti-6Al-4V alloy as an example, as well as on the kinetics and mechanisms of fatigue failure. The prospects and problems of the practical application of UFG Ti materials in medicine and aircraft engine construction are discussed.

Keywords: titanium alloys; ultrafine-grained structure; fatigue behavior; crack growth rate; fatigue failure mechanisms; engineering application



Citation: Semenova, I.P.; Modina, Y.M.; Stotskiy, A.G.; Polyakov, A.V.; Pesin, M.V. Fatigue Properties of Ti Alloys with an Ultrafine Grained Structure: Challenges and Achievements. *Metals* **2022**, *12*, 312. <https://doi.org/10.3390/met12020312>

Academic Editor: Thomas Niendorf

Received: 29 December 2021

Accepted: 7 February 2022

Published: 10 February 2022

Publisher's Note: MDPI stays neutral with regard to jurisdictional claims in published maps and institutional affiliations.



Copyright: © 2022 by the authors. Licensee MDPI, Basel, Switzerland. This article is an open access article distributed under the terms and conditions of the Creative Commons Attribution (CC BY) license (<https://creativecommons.org/licenses/by/4.0/>).

1. Introduction

Fatigue is one of the key mechanical characteristics of metals and alloys. It is associated with a gradual accumulation of strain/damage in a material, which leads to the formation of cracks, their propagation, and eventually material failure. Therefore, among the most important properties of structural materials, fatigue holds a special place, and increasing the resistance to fatigue failure is a very important task for the use of new materials in medicine and engineering.

The development of methods of deformation treatment of metals and alloys, in particular, the severe plastic deformation (SPD) techniques, has resulted in the design of materials with ultrafine-grained (UFG) and nanocrystalline (NC) structures [1–3]. It is known that the principal factor influencing the nucleation and propagation of fatigue cracks is undoubtedly the microstructure of a material. One of the structural parameters that mechanical properties strongly depend on is grain size [4,5]. The well-known Hall–Petch Equation (1) describes a tendency common to most materials: strength increases with decreasing grain size. It is also used for the endurance limit [4].

$$\sigma_f = \sigma_{if} + K_f \times d^{-1/2} \quad (1)$$

where σ_{if} and K_f are constants for the material. As grain size decreases, it becomes more difficult for dislocations to move in a material, and grain boundaries start to play an increasing role in plastic deformation, since they are an efficient sink/source for defects, as well as a barrier for dislocation glide [4]. However, this law is not always true. Since, at a very small grain size, grain boundaries occupy a considerable fraction of the volume, the action of certain deformation mechanisms is impeded, and as a result, the mechanical properties

turn out to be different from the material's expected properties. The law's nonlinearity is also exhibited when the nanometric grain size is reached [6]. Thus, during the grain refinement of metals and alloys the fatigue characteristics may increase disproportionately to the ultimate tensile strength (*UTS*) and may even decline, or at least not improve compared to the initial structure.

The experimental database on the fatigue of ultrafine-grained (UFG) materials has been intensively expanding to date. The most significant research in the area of fatigue was performed on submicrocrystalline (SMC) polycrystals (grain size 200–300 nm) produced by SPD [7–9]. Such a severe deformation produces a typical UFG structure with a grain size about 200 nm in Cu and its alloys. Enhancement of high-cycle fatigue was systematically observed, together with an increase in tensile strength (static strength). Many publications proved that the most impressive strengthening, to 200–300%, was normally achieved under a relatively small strain equivalent, of about $e = 1.15$, where low-angle grain boundaries prevailed in the microstructure [10,11]. Further deformation and the creation of high-angle grain boundaries associated therewith resulted in only minor additional strengthening.

Analysis of these research results leads to the following general observations, summarized in [4,12–14], that are based on the commonly accepted approach to fatigue life. Grain refinement, leading to the strengthening of metals and alloys, results in improved fatigue characteristics in the high-cycle fatigue (HCF) regime, i.e., an increase in the endurance limit of smooth fatigue specimens subjected to constant stresses or amplitude cyclic loads. It is normally considered that the positive effect on high-cycle fatigue life occurs due to the inhibition of cracks that nucleate on the surface as a response to higher static strength and cyclic endurance limit. In contrast to this trend, resistance to fatigue damage normally declines during grain refinement in the low-cycle fatigue (LCF) regime or during tests of the crack growth resistance, especially in the range of a low stress intensity ΔK in the near-threshold regime. An obvious increase in the resistance to fatigue failure with decreasing grain size is attributed to the possible effects of decreasing efficient moving force, due to microstructural changes in the crack path and the concomitant possibility of contact between irregularities on the crack surface [15,16].

At the same time, the results of tests of UFG materials performed in different laboratories often have a contradictory character. On the one hand, this is related to the fact that the endurance limit of metallic materials strongly depends on the geometry, size, and surface quality of the specimens, as well as on the test conditions [5]:

- loading pattern: bending, rotational bending, cyclic tension, torsion;
- cycle symmetry $R = \sigma_{\min}/\sigma_{\max}$;
- load application frequency, f [Hz];
- test temperature and environment.

On the other hand, for complex alloys, having a multiphase structure, grain-boundary strengthening may be disguised by such mechanisms as solid-solution hardening and dislocation strengthening, while the redistribution of phases and alloying elements may lead to a brittleness of grain boundaries and a decline in the alloy's ductility at room temperature [17]. For example, for the Al alloys 5056 and 6061, the increase in fatigue strength after processing by equal-channel angular pressing (ECAP) was insignificant. Thus, in spite of considerable efforts, the relation to the microstructure formed in the process of SPD is not always obvious.

The fatigue properties of Ti polycrystals with different purities and grain sizes were investigated in detail in [18–24]. In particular, Turner and Roberts [18] demonstrated convincingly that the endurance limit grew considerably with grain size, decreasing from 100 to 9 μm . In addition, the endurance limit/ultimate tensile strength ratio (σ_f/UTS) that is sometimes used as an approximate empirical measure of engineering cyclic properties was over 0.5 [18]. This assumes that grain size reduction to the nanoscale may lead to a further enhancement of titanium's fatigue characteristics. However, it should be kept in mind that improving static strength and even endurance limit during stress-controlled tests does not

ensure improvement of cyclic properties during strain-controlled tests. In fact, stress and the concept of the fatigue estimation based on strain are often inconsistent, because if cyclic strength at a constant applied load is improved, the load-carrying capacity of a material is often sacrificed, due to the loss of ductility [24].

The object of analysis in the present work is Ti and its alloys, which are widely applied in different industries, such as aviation, medicine, and mechanical engineering. The formation of an ultrafine-grained structure in these, by means of SPD processing, and enhancement of their mechanical properties, including fatigue ones, has been demonstrated in many studies over the past 20 years, and summarized in overview papers [25–28]. The aim of this overview is to analyze the fatigue properties achieved to date in Ti alloys subjected to SPD. In Section 1, we examine the fatigue behavior of commercially pure (CP) Ti in the UFG state and the methods increasing its fatigue resistance. Section 2 reports on the recent studies of the fatigue properties of two-phase Ti alloys, using the popular alloy Ti-6Al-4V as an example. It is obvious that an evaluation of the fatigue crack growth rate is necessary for a deeper understanding of the fatigue properties of UFG materials, but information about the kinetics and mechanisms of the fatigue failure of UFG Ti alloys is, to date, very scarce. Section 3 presents an analysis of some publications in this research area, with UFG Ti and the Ti-6Al-4V alloy as examples. In recent years, papers have started to appear, dealing with the prospects of the practical application of UFG Ti materials in medicine (prosthetics) and aviation, but the transition from laboratory samples to real products requires solving a number of scientific and technical problems, briefly specified in Section 4.

2. Fatigue Behavior of CP Ti Produced by Severe Plastic Deformation

The first attempt to evaluate the fatigue properties of Ti with a grain size below 0.5 μm was made in [29,30]. An increase was reported in the fatigue resistance of CP Ti (Grade 2) processed by ECAP with subsequent thermomechanical treatment. Depending on the processing regime, three types of nanostructured state were produced in Ti, with a grain size from 250 to 150 nm, differing in the mean grain size and grain shape. It was shown that highest fatigue limit was achieved in Ti with a fragmented structure, which had mutually misorientated regions/subgrains with low-angle and medium-angle deformation-induced boundaries, with a mean grain size of 0.15 μm , amounting to 482 MPa, in comparison to 238 MPa for its coarse-grained counterpart. The σ_f/UTS ratio reached the highest values (0.57) in the specimens with the most homogeneous and practically equiaxed structure [29].

Figure 1 shows a diagram demonstrating the relationship between UTS and endurance limit for CP Ti in different structural states, as reported in the papers by Kolobov, Stolyarov, Vinogradov, and others back in the early 2000's [29–32].

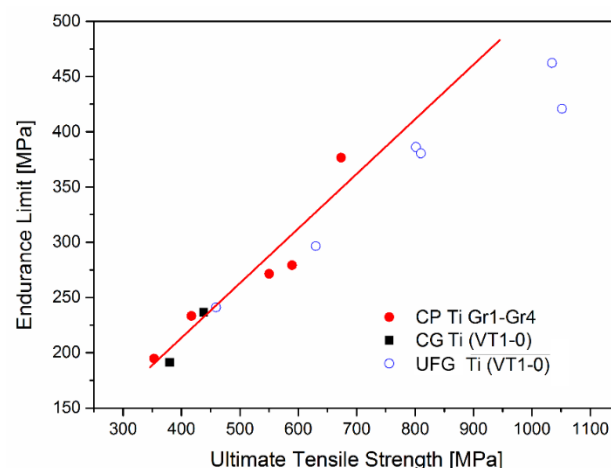


Figure 1. Relationship between UTS and endurance limit for CP Ti in different structural states adapted from [32] (VT1-0 is a Russian analogue of grade 2).

According to [31], the endurance limit of Grade 2 Ti reaches 380 MPa, which is considerably higher than that of CP Ti, with a fine grain size of 9 μm —225 MPa according to [18], and Ti with a grain size of 25 μm —238 MPa according to [29]. Nevertheless, the σ_f value is more modest, in comparison to the endurance limit of 482 MPa reported in [29,30], for ECAP-processed Ti with a so-called fragmented equiaxed structure, according to [30]. This value of 480 MPa is still lower than that of the popular alloy Ti-6Al-4V ELI (515 MPa) [33].

Vinogradov et al. [31] showed the results for the plastic-strain controlled fatigue properties of UFG CP Ti were similar to the results obtained earlier for ECAP-processed Cu, with an almost equiaxed grain structure in [9,14]. Notable, were the absence of progressive softening for all strain amplitudes and a pronounced saturation stage.

Contrary to Agnew and Weertman [34] and Höppel et al. [35], who reported that such UFG materials as copper and Al alloys exhibited a significant degradation of cyclic properties with controlled strain, Ti does not exhibit any decline in its fatigue characteristics during cyclic testing at a constant value of plastic strain, as testified by almost the same behavior of the Coffin–Manson graph in the fine-grained and coarse-grained states (Figure 2). This result agrees well with the fact that in UFG Ti, unlike in ECAP-processed Cu according to [31], there were no significant microstructural changes after testing, in particular, to grain coarsening.

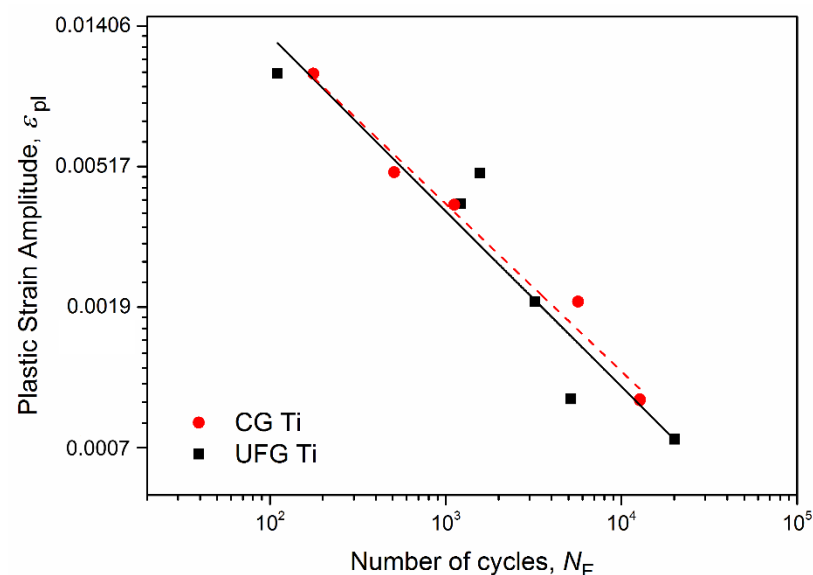


Figure 2. Cyclic stress–strain plot for UFG and coarse-grained Ti reprinted with permission from ref. [31]. Copyright 2001 Elsevier.

A large number of studies on fatigue have been performed on UFG Ti of different purities (Grade 2 and Grade 4) produced by ECAP in combination with different thermo-mechanical treatments. These processing methods enable producing bulk billets, which facilitates the fabrication of standard specimens for fatigue tests. For example, for UFG VT1-0 (Grade 2 Ti analogue) produced by ECAP in combination with cold rolling, UTS increased by a factor of more than 2.5, whereas the endurance limit did not exceed 400 MPa ($\sigma_f = 280$ MPa for coarse-grained VT1-0) [30]. The researchers attributed this to the reduced plasticity margin after cold rolling, conditioned by such features of the formed UFG structure as the critical density of dislocations, a high fraction of low-angle dislocation boundaries, and a high level of internal elastic stresses.

An increase in ductility without a considerable decline in strength was achieved due to the optimization of the regimes of a combined deformation treatment. In [36], the process of producing UFG Grade 4 Ti rods included a combination of ECAP and subsequent drawing with intermediate annealing. The mechanical properties reached very high values, with the

preservation of a satisfactory ductility: UTS 1235 MPa and elongation 11%. The specimens were tested under cyclic tension with a controlled stress and the cycle asymmetry coefficient R ($\sigma_{\min}/\sigma_{\max}$) = 0.1. The endurance limit of UFG Grade 4 Ti was 620 MPa on the basis of 10^6 cycles, which is higher than the fatigue strength of conventional Ti in the coarse-grained state by a factor of almost 1.5 (350 MPa after 10^6 cycles according to [37]) and is at the level of the Ti-6Al-4V alloy.

A high strength and retained enhanced ductility were achieved in UFG Ti rods by using low-temperature annealing [38]. In [39], for Grade 4 Ti rods produced by ECAP in combination with drawing and annealing at 350 °C for 6 h, the endurance limit of the specimens grew from 590 to 610 MPa, as a result of an increase in strength to 1250 MPa and ductility from 11 to 13%. Here, the tests were performed on the basis of 10^7 cycles in a more rigid symmetrical cycle $R = -1$, unlike in [36]. According to the authors, the extraordinary simultaneous increase in strength and ductility after 6 h of annealing may have been associated with recovery processes of non-equilibrium boundaries, which were accompanied with ordering of their structure and a decrease in the dislocation density, and with impurity segregation formation in the boundaries and near-boundary areas.

In [40], the possibility was demonstrated of improving the fatigue strength of Grade 4 Ti by means of using warm rolling (WR) in contrast to cold drawing (D), due to a decrease in the structural anisotropy in the transverse and longitudinal sections, and the formation of more equiaxed grains with a large fraction of high-angle boundaries. Fatigue tests were performed on smooth specimens under similar conditions of rotational bending; the testing base was $N_F = 10^7$ cycles. The higher strength (1310 MPa) of the rods processed by ECAP+WR, with the preservation of a good ductility, provided a higher endurance limit (up to 640 MPa) in comparison to the ECAP+D condition (610 MPa), where the strength did not exceed 1235 MPa (Figure 3).

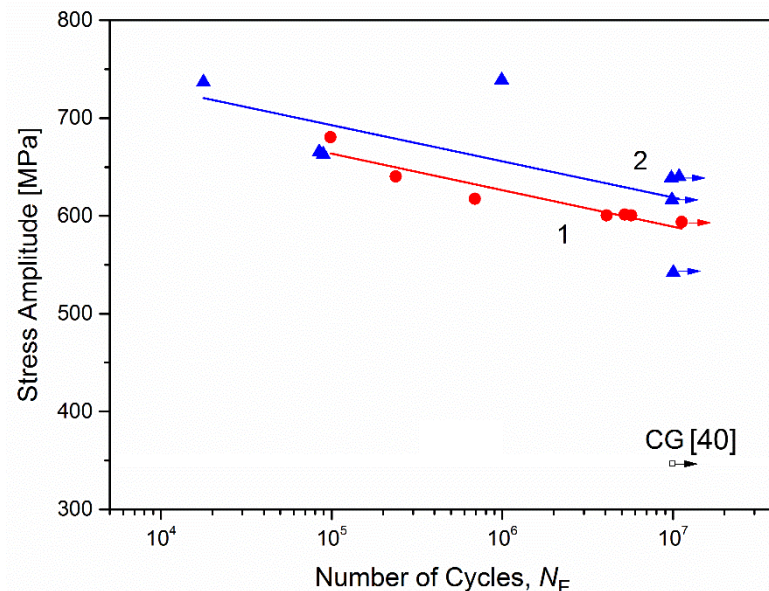


Figure 3. Number of cycles to failure vs. stress amplitude for smooth specimens cut out of Grade 4 Ti rods in as-received condition, after ECAP+Drawing (curve 1), and after ECAP+Warm Rolling (curve 2).

It is evident that the increase in the endurance limit of the UFG Ti rods was achieved as a consequence of a large increase of flow stress and static strength, resulting from grain refinement. The results obtained in that work showed that the fatigue strength of UFG Ti was noticeably influenced by the ratio between the strength and ductility of the material, which in their turn depended on such structural features as grain size and shape, and the condition of grain boundaries. As was shown in [40], rods processed by ECAP+D exhibited

a high degree of structure anisotropy in the transverse and longitudinal directions, which was characterized by elongated-shape grains and a large fraction low-angle boundaries in the longitudinal structure of the rods, due to the use of cold drawing after ECAP.

We should also mention the results from a study of the fatigue properties of CP Ti produced using ECAP-Conform (ECAP-C), which is a more productive variation of the well-known ECAP process that enables producing long-length rods at lower deformation temperatures (200 °C) than the ECAP process (400–450 °C) [41]. As was demonstrated above, the endurance limit does not always vary in accordance with expectations from the level of static strength. This may be related to the low capacity of the materials for plastic flow, i.e., early strain localization [1]. A study [41] examined the effect of the strain degree of ECAP-C and following drawing. Rods were produced by ECAP-C for six passes, followed by drawing with 75% reduction (regime 1), and by ECAP-C for 10 passes, followed by drawing with 75% reduction (regime 2). Study of the fatigue properties of the UFG Grade 4 Ti rods, with the mechanical properties of $UTS = 1240$ MPa and $\delta = 12\%$, produced via regime 1, revealed that the endurance limit of the specimens was 590 MPa, in comparison to 380 MPa for the as-received condition. An increase in yield stress and UTS to 1220 and 1290 MPa (regime 2), respectively, raised the endurance limit to 610 MPa.

A marked increase in the fatigue resistance of CP Ti was achieved by applying methods other than ECAP, e.g., multiaxial forging [42] or hydrostatic extrusion [43]. Nanocrystalline Ti produced by hydrostatic extrusion ($d = 50$ nm) showed a 75% increase in fatigue strength (from 160 to 280 MPa) as compared to CG Ti, used as a reference, with a grain size of 20 μm . Multiaxial forging produced a microstructure and properties similar to those produced by ECAP processing.

It is obvious that the critical parameter of the UFG structure in Ti for increasing its fatigue strength is grain size, and its reduction to 100 nm ensures a considerable enhancement of static strength. At the same time, the ductility level of UFG Ti also plays an important role in fatigue resistance; in particular, the formation of high-angle boundaries promotes the grain-boundary processes involved in deformation, e.g., dislocation accumulation at grain boundaries, while the equiaxed grain shape contributes to the uniformity of plastic flow and reducing the probability of early strain localization.

It is known that actual products and structures may have different geometrical features, which may affect their fatigue life. In particular, in medicine, threaded pins and screws of different types are used. For such products, a very high strength is not always required, which often leads to a decline in ductility and fracture toughness, and an increase in sensitivity to stress raisers [44]. Therefore, the practical application of UFG Ti, e.g., in dental traumatology, calls for the examination of notch fatigue properties.

For example, in [45] the fatigue life and notch sensitivity of ultrafine-grained pure Ti produced by ECAP was investigated. The ECAPed Ti showed a significant improvement in its high cycle fatigue limit (by a factor of 1.67), but its notch sensitivity was increased.

A study [46] examined the effect of additional design factors, such as notch sharpness and notch surface quality, on fatigue resistance. As shown in Figure 4, the endurance limit of smooth specimens on the basis of 10^7 cycles was 610 MPa (curve 1 in Figure 4). A notch is known to reduce the endurance limit of a material, and the notch value depends on its height h and radius ρ . It can be seen from Figure 4 that notched specimens having the largest stress concentration of $\alpha_t = 4.4$ could withstand a load with a maximum stress of 220 MPa for 10^7 cycles (curve 2). With decreasing concentration factor α_t to 3.3, the maximum stress grew to 295 MPa (curve 4). Thus, a decrease in the notch radius considerably reduces the endurance limit of UFG Grade 4 Ti, due to an increase in the stress concentration factor. Such regularity is also typical for Ti with a conventional coarse-grained structure [37].

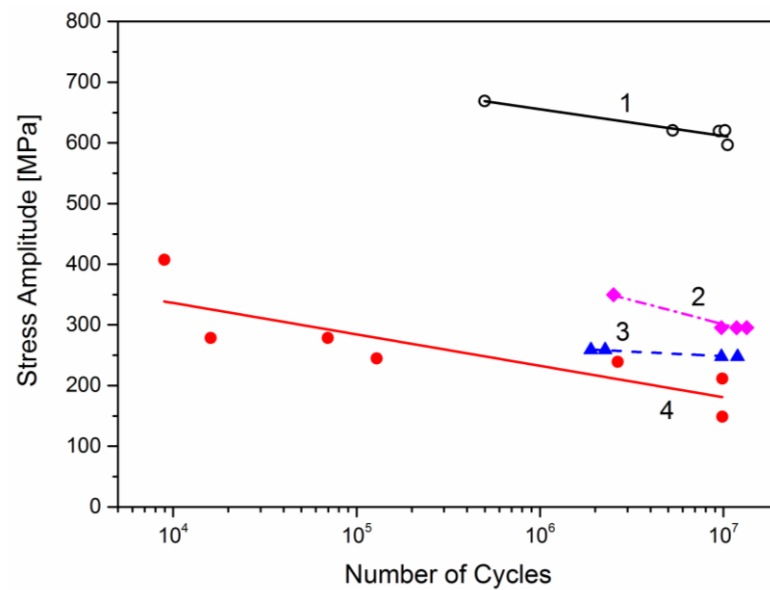


Figure 4. Dependence of the number of cycles to failure on the cycle stresses amplitude for specimens with different notch geometry: 1—smooth specimens; 2—notched specimens $\alpha_t = 4.4$; 3—notched specimens $\alpha_t = 3.9$; 4—notched specimens $\alpha_t = 3.3$ reprinted with permission from ref. [46]. Copyright 2009 Elsevier.

Meanwhile, the endurance limit of notched strengthened UFG Ti is slightly lower than the endurance limit of conventional coarse-grained Ti (220 and 230 MPa at $R = -1$) and comparable to the endurance limit of both smooth and notched specimens of the medical alloy Ti-6Al-4V ELi (290/610 MPa) (Figure 5).

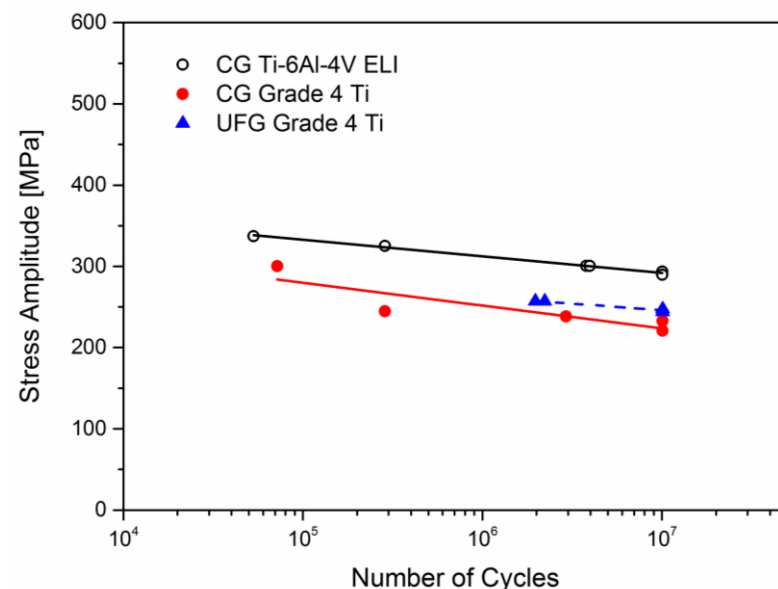


Figure 5. Dependence of the number of cycles to failure on the stress amplitude for UFG and CG Ti Grade 4, in comparison with the medical alloy Ti-6Al-4V ELI.

Another interesting effect should be mentioned here: the possibility of improving the fatigue resistance of notched specimens by means of increasing the notch surface quality (namely, by reducing the surface roughness) through acid etching, which is widely applied in the manufacture of dental implants, in order to remove various types of impurities and oxides [47]. This fact was demonstrated in a recent paper [48]. The surface topography obtained as a result of acid treatment may be adjusted by using a preliminary treatment, a

mixture of acids, and various etching temperatures and times [48]. For example, a study [49] investigated the effect of etching on the mechanical behavior of UFG Ti. It was shown that etching with a mixture of HNO₃ and HF acids for 20 min did not impair the mechanical properties of UFG Ti, but on the contrary somewhat increased its tensile strength, due to the formation of a homogeneous porous structure on the surface of the specimens, in comparison to machining [49]. The same regime and acid mixture were used by the authors to etch the notch surface of the fatigue specimens. A change in the surface topography with a decrease in the relative value of surface microdefects resulted in the localization of smoothing near the defects, which in its turn increased the time of crack nucleation.

It follows from the presented data that the structural refinement achieved through a set of measures including SPD processing by ECAP and subsequent thermomechanical treatment is very efficient for producing high, and even record-breaking, fatigue characteristics in CP Ti. Grain size is a critical structural parameter of CP Ti and its reduction to 0.1–0.2 μm increases the material's strength and, consequently, the crack nucleation, due to an increase in the extent of the boundaries. Grain size reduction to below 100 nm may lead to early strain localization, as was demonstrated previously for several nanostructured metals. Therefore, this lower ductility in comparison to the coarse-grained state does not always provide as great an increase in fatigue life as one could expect from grain size reduction. Grain shape may also influence fatigue resistance; therefore, an increase in the fraction of equiaxed-shape grains in combination with their high-angle boundary misorientation contributes to the uniformity of plastic flow and to reducing the probability of early strain localization.

3. Fatigue Behavior Features of the Ultrafine-Grained Ti-6Al-4V Alloy

Traditionally, the increase in the fatigue characteristics of Ti alloys is achieved by means of increasing *UTS* through alloying or varying the structural and phase composition by thermal or thermomechanical treatments that may produce microstructures of different morphologies (equiaxed, lamellar, mixed, etc.) [50–52]. As shown previously, the Ti-6Al-4V alloy exhibits the best resistance to high-cycle fatigue (10⁷ cycles) when a mixed globular and fine-lamellar microstructure is formed, in contrast to equiaxed and lamellar structures [53]. A microstructure of this type is often referred to as bimodal or duplex.

Among two-phase Ti alloys the Ti-6Al-4V alloy has been the most studied in publications over the last 20 years, and most of these publications show that the formation of a submicrocrystalline or ultrafine-grained structure leads to an increase in the endurance limit at room temperature [27,28,40,54–60].

For example, a study [58] demonstrated an increase in the strength and endurance of VT1-0, VT6 (Russian analogue of Ti-6Al-4V alloy) and VT22 (Ti-5.1Al-5.4V-4.9Mo-1.0Cr-1.0Fe-0.08Si) in the UFG state produced by multiaxial isothermal deformation. However, the absolute increment in the endurance limit for these materials was 70, 110, and 105 MPa, respectively, which may have been associated with the presence of the highly ductile β-phase in the alloys, unlike in pure Ti, and also with an increase in energy spent on crack nucleation, where the difference between the energies of crack nucleation and crack propagation raises the total fatigue resistance in alloys in comparison to Ti [57,58]. In alloys, in contrast to Ti, a decrease is observed in the contribution of strain hardening in the process of SPD, which is associated with the increased contributions of solid-solution strengthening and precipitation hardening (the decomposition of a supersaturated solid solution of the β-phase as dispersed particles of a secondary α phase).

Studies [55,56] investigated in detail specimens of the Ti-6Al-4V ELI alloy in the CG state and in the UFG state after ECAP processing in high-cycle and low-cycle fatigue regions at room temperature. It was shown that the behavior of the alloy in both investigated states in the low-cycle fatigue region corresponded quite well to the Coffin–Manson rule, Equation (2)

$$\Delta\varepsilon_{pl}/2 = \varepsilon'_f (2N_f)^c \quad (2)$$

where $\Delta\varepsilon_{pl}/2$ is the plastic strain amplitude, ε'_f is the fatigue ductility coefficient, $2N_f$ is the number of cycles to failure, and c is the fatigue ductility exponent. These works demonstrated that in the investigated plastic strain amplitude range from 10^{-2} to 2×10^{-5} the fatigue ductility exponent c remained practically identical for the CG and UFG materials, which had previously been found for UFG Ti [31]. Meanwhile, the total fatigue life of the UFG alloy in the Wöhler curves was higher than that of the CG alloy, and the curves did not intersect in the region of the investigated strains, whereas the increment in the endurance limit of the UFG alloy was about 15% [56].

It should be noted that the UFG Ti-6Al-4V alloy has a reduced fatigue resistance in the region of low-cycle tests in comparison its coarse-grained state, which is related to a certain loss in ductility and an increased YS value [61]. In the Wöhler's curves in the high stress amplitude region during low-cycle tests, the endurance limit values for the UFG alloy were larger than those for the CG alloy [56]. Such results were reported in [60], where tests were conducted in a wide range of stress amplitudes, from 700 to 1050 MPa, at a frequency of 5 Hz. However, when increasing the number of test cycles, the slope of the fatigue curve in the UFG state was greater than that for the CG alloy, which may indicate a more intense softening in comparison with a coarse-grained analogue.

In [40], fatigue tests of the specimens from the commercial alloy Ti-6Al-4V (Russian analogue—VT6) were carried out under rotational bending with a frequency of 50 Hz and a symmetrical loading cycle ($R = -1$). It was found that the alloy's high strength and ductility (1550 MPa and 12%), produced by ECAP in combination with extrusion and annealing at 500 °C, raised the endurance limit from 600 to 740 MPa on the basis of 10^7 cycles (Figure 6). The endurance limit obtained in that paper for the VT6 alloy under rotational bending was higher than previously achieved. For example, a study [54], where fatigue tests were performed with the asymmetry coefficient $R = 0$ on specimens from the conventional coarse-grained VT6 alloy and the submicrocrystalline VT6 alloy produced by 'abc' multiaxial deformation, reported an increase in endurance limit of about 17%.

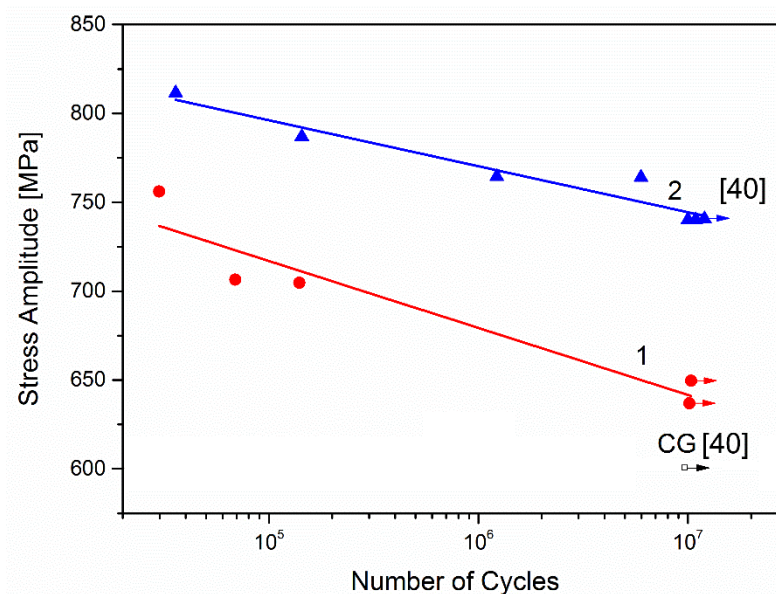


Figure 6. Number of cycles to failure vs. stress amplitude (rotational bending, $R = -1$, $f = 50$ Hz) for smooth samples from the conventional and nanostructured Ti-6Al-4V alloy. Where CG—Bimodal Ti-6Al-4V, 1—Fine Grained Ti-6Al-4V, 2—UFG Ti-6Al-4V.

Another study [62] showed that the formation of a UFG state in the Ti-6Al-4V alloy enabled raising the strength characteristics to 1300 MPa after 'abc'-deformation and to 1500 MPa after subsequent rolling, which is 25 and 40% higher than for the CG state, while simultaneously raising the material's ductility and toughness, including the fatigue limit,

which was determined using the ‘stairs’ method for 2×10^7 loading cycles and found to be 20% higher in the UFG state than in the CG state.

It is known that in the case of strengthened Ti alloys the σ_f/UTS ratio normally varies, from 0.4 for a coarse-grained lamellar structure, to 0.62 for a fine-grained globular $\alpha + \beta$ structure [37]. The table below summarizes the data for the Ti-6Al-4V alloy and CP Ti produced by different SPD processes.

To compare the data on the fatigue properties of CP Ti of different purities and the Ti-6Al-4V alloy in the fine-grained and UFG states, Figure 7 shows the dependence of endurance limit on UTS .

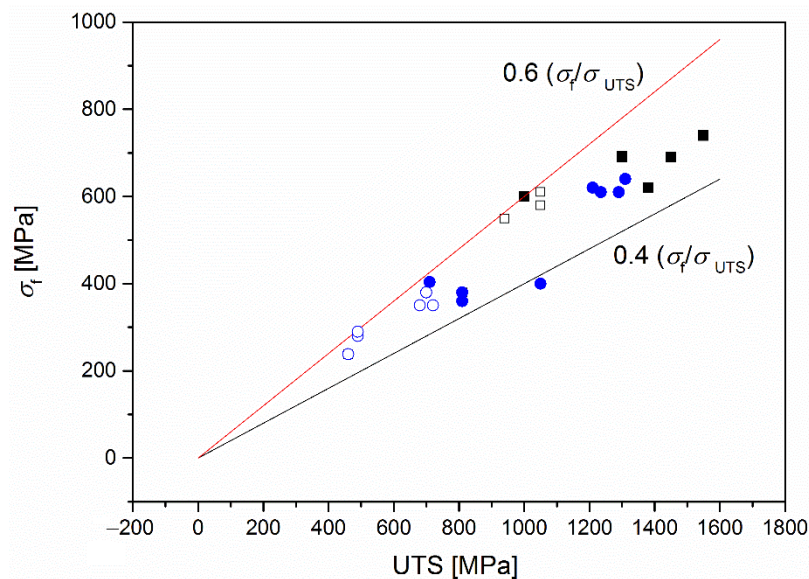


Figure 7. Ratio between UTS and endurance limit (σ_f) for Ti Grade 4 CP Ti and the Ti-6Al-4V alloy in CG and UFG states ($\sigma_f/UTS = 0.6$ for annealed; $\sigma_f/UTS = 0.4$ for heat-strengthened Ti alloys) adapted from [37].

It can be seen from Table 1 and Figure 7 that the σ_f/σ_{UTS} ratio for Ti-based materials strengthened by SPD varies from 0.47 to 0.58, i.e., does not go beyond the value limits for conventional annealed and heat-strengthened Ti alloys [37]. This conclusion is important for the different engineering applications of UFG Ti alloys.

On the other hand, it is also clear that approaches aimed only at increasing monotonous strength are common, since the fatigue ratio σ_f/σ_{UTS} remains practically unchanged following a linear correlation between these two parameters. Probably, for the most efficient enhancement of the endurance of materials, the character of the σ_f/σ_{UTS} ratio needs to be changed; this can be attempted only by controlling the material structural parameters that influence, not only strength, but also ductility.

Table 1. Mechanical properties of Ti alloys in different states.

Alloy	Ref	State	Average Value of UTS (MPa)	σ_f (MPa)	σ_f/UTS
Ti-6Al-4V ECAP+extrusion $R = -1$ rotation bending, 10^7	[60]	CG bimodal UFG	1050 1450	610 690	0.58 0.47
Ti-6Al-4V ELI ECAP+extrusion $R = -1$ rotation bending, 10^7	[40]	CG equiaxed UFG	1000 1550	600 740	0.60 0.54
Ti-6Al-4V ELI ECAP+extrusion tension-compression $R = -1, 10^6$	[56]	CG equiaxed UFG	940 1380	550 620	0.59 0.45
Ti-6Al-4V Multi-axial forging (MAF) bending, $R = 0, 2 \times 10^7$	[54]	Fine grained SMC	1050 1300	580 690	0.55 0.53
Ti-6Al-4V Multi-axial forging bending, $R = 0, 2 \times 10^7$	[58]	Fine grained SMC	1050 1300	580 693	0.55 0.53
ECAP Ti Gr2 tension-compression $R = -1, 10^6$	[31]	CG UFG	460 810	238 380	0.52 0.47
ECAP VT1-0 tension-compression $R = -1, 10^6$	[30]	CG UFG	490 1050	280 400	0.57 0.38
ECAP VT1-0 tension-compression $R = -1, 10^6$	[29]	CG UFG	460 710	238 404	0.52 0.57
MAF CP VT1-0 bending, $R = 0$ 2×10^7	[58]	CG UFG	490 810	290 360	0.59 0.44
ECAP+D Ti Grade 4 $R = -1$ rotation bending, 10^7	[41]	CG UFG	700 1290	380 610	0.54 0.47
ECAP+D Ti Grade 4 tension-compression $R = -1, 10^6$	[36]	CG UFG	720 1210	350 620	0.49 0.51
ECAP+D Ti Grade 4 $R = -1$ rotation bending, 10^7	[40]	CG UFG	680 1235	350 610	0.51 0.49
ECAP+WR Ti Grade 4 $R = -1$ rotation bending, 10^7	[40]	CG UFG	680 1310	350 640	0.51 0.49

4. Kinetics and Mechanisms of the Fatigue Failure of UFG Ti Alloys

To gain a deeper understanding of the fatigue properties of UFG materials, it is necessary to evaluate the fatigue crack growth rate. Specifically, Estrin and Vinogradov in [4] and several other researchers in [6,16,63–69] demonstrated that UFG materials normally have lower threshold values of the stress intensity factor ΔK and a higher crack propagation rate in the stationary regime compared to coarse-grained materials. Similar results should be mentioned, obtained by Hübner et al. [63] for CP Al, Chung et al. [16] for the

heat-treatable UFG aluminum alloy AA6061, Meyers et al. [64] for the Al-Mg alloy AA6063, Kiessling et al. [65], and Hanlon et al. [6] for Ti.

The low strength of UFG materials in the low-cycle fatigue region was attributed by researchers in [4,13,15] to the lower tortuosity of a propagating crack, leading to a decrease in the fracture surface roughness and to a relatively well-developed cyclic plastic strain at the crack tip. However, a certain divergence from these conclusions was found during the fatigue testing of UFG magnesium alloy AZ31 [13]. It was shown in [70] that the difference in the crack path was related to grain size. For example, if the grain size was below 1 μm , intercrystalline crack propagation was observed; if the grain size was above 1 μm , a transcrystalline one.

A study [6] revealed a dependence of the fatigue crack growth rate on grain size in Grade 2 Ti with grain sizes of 22 and 0.5 μm . In the whole range of the threshold values of the stress intensity factor ΔK , the crack growth rate da/dN was higher for UFG Ti than for its CG counterpart (Figure 8). Grain size reduction leads to a decrease by a factor of 2.5 in the threshold value ΔK_{th} . Figure 8 demonstrates the same crack propagation stages as for conventional polycrystals; namely, slow crack propagation in the near threshold region and an intermediate stage corresponding to stable crack growth.

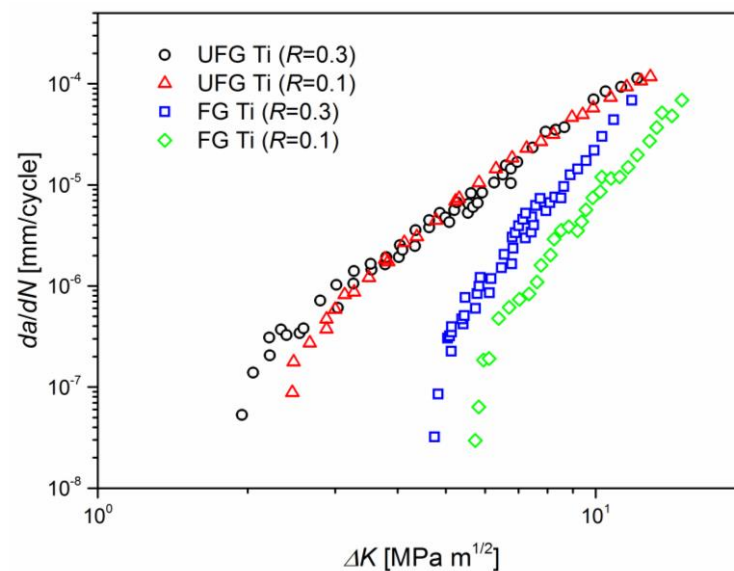


Figure 8. Variation in fatigue crack growth rate, as a function of ΔK for commercially pure fine-grained (FG) and UFG Ti at a fatigue frequency of 10 Hz at room temperature reprinted with permission from ref. [6]. Copyright 2005 Elsevier.

As is well known, Paris's law, Equation (3), is normally applied for crack propagation in stage 2 [71].

$$dl/dN = C(\Delta K)^n \quad (3)$$

where N is the number of loading cycles, l is the crack length, n is a material's constant, and ΔK is the stress intensity factor range that is found from the Formula (4).

$$\Delta K = Y\Delta\sigma\sqrt{\pi l} \quad (4)$$

where $\Delta\sigma$ is the difference between the maximum and minimum applied stresses, and Y is the coefficient depending on the specimen's geometry.

In [72], kinetic diagrams of fatigue failure were obtained for Grade 4 CP Ti processed using ECAP-Conform with a grain size of 0.35 μm . ECAP-Conform processing increases the number of loading cycles up to the emergence of a fatigue crack, which is associated with a higher strength of UFG Ti. It was found that the kinetic diagram of fatigue failure for Ti processed by ECAP-Conform was located below the fatigue failure curve for the

material in the initial condition. From this it follows that at the same value of stress intensity factor range (ΔK), the fatigue crack propagation rate in Ti after ECAP-Conform processing should be lower than that in the initial condition. This is an unusual result and somewhat contradicts the results obtained for Grade 2 Ti in [6]. The straight-linear segments of the kinetic diagrams of fatigue failure for Grade 4 Ti in the initial CG condition and after ECAP-Conform processing are well described by the Paris Equation (5) for Ti in the initial condition.

$$dl/dN = 4.31 \times 10^{-11} \Delta K^{3.5} \quad (5)$$

and after ECAP-Conform processing in Equation (6)

$$dl/dN = 2.19 \times 10^{-15} \Delta K^{6.3} \quad (6)$$

It can be seen from Equations (5) and (6) that in the case of Grade 4 Ti in the initial condition, the coefficient n in the Paris equation equals 3.5, while in the case of ECAP-Conform processing it is two times higher and equals 6.3. The latter may indicate [73] that Grade 4 Ti processed by ECAP-Conform has an increased sensitivity to overloads (a single-time increase in ΔK) compared to the initial condition. In other words, short-time overloads in Ti processed by ECAP-Conform cause a larger increase in the fatigue crack propagation rate than in Ti in the initial condition. Thus, on the one hand, UFG Grade 4 Ti exhibits an extraordinary decrease in crack propagation rate in comparison to the coarse-grained state, and on the other hand, a tendency is observed for the crack propagation rate to increase, on the condition that there is a short-term increase in ΔK , in accordance with the Paris equation.

To date, there has been very limited information about the study of crack propagation rate in two-phase Ti alloys with a UFG structure. The Ti-6Al-4V alloy exhibits a tendency, similar to that of many investigated materials, for the crack propagation rate to increase at the same value of the stress intensity factor range ΔK . In particular, a study [74] investigated the kinetics and mechanisms of the fatigue failure of Ti-6Al-4V alloy. The alloy's UFG structure was produced by ECAP and had a mean α -phase grain size of 0.25 μm , in comparison to the initial equiaxed structure with a grain size of 15 μm . It was demonstrated that under the same loading conditions (ΔP), the life (the number of cycles to failure) of specimens of the alloy in the initial condition was higher than that for the alloy's ECAP-processed condition. With decreasing cycle stress, the number of cycles to the nucleation of a fatigue crack decreases. However, the alloy's condition has a small effect on this characteristic.

The straight-linear segment in the kinetic diagrams of fatigue failure for the VT6 alloy is approximated by the Paris Equation (7) for CG alloy, and Equation (8) for UFG alloy:

$$dl/dN = 7.6 \times 10^{-12} \Delta K^{3.63}, \quad (7)$$

$$dl/dN = 2.5 \times 10^{-11} \Delta K^{3.30} \quad (8)$$

It was shown that the fatigue-crack propagation velocity in the alloy with a UFG structure was somewhat higher than in the sample with a CG structure at the same ΔK . However, the values of coefficient n in the Paris equation were very close to one another (3.6 and 3.3), which points to the identical sensitivity of the alloys to cyclic overloads [73].

Examining the research data for Ti and the Ti-6Al-4V titanium alloy, one can assert an ambiguous effect of grain refinement on the crack propagation rate. Apparently, the crack propagation mechanisms are largely influenced by such UFG structure parameters as dislocation type, grain (cell) size, and the characteristics of the second-phase particles, including their average size and spatial distribution, as well as the texture formed [4].

Therefore, let us consider the results from the study of the fracture mechanisms of Ti and its alloys during fatigue tests, in both low-cycle and high-cycle regions, which were separately addressed in several papers.

For example, a study [31] examined the character of the fracture surface relief after LCF tests of UFG Grade 2 Ti under strain control for two plastic strain amplitudes in different regimes -5×10^{-3} and 7.5×10^{-4} . The fracture surface morphology of the specimens was characterized, with a honeycomb location of dimples with a distinct elongated shape in the form of ‘fish scales’, which is on the whole characteristic of lamellar fracture (Figure 9).

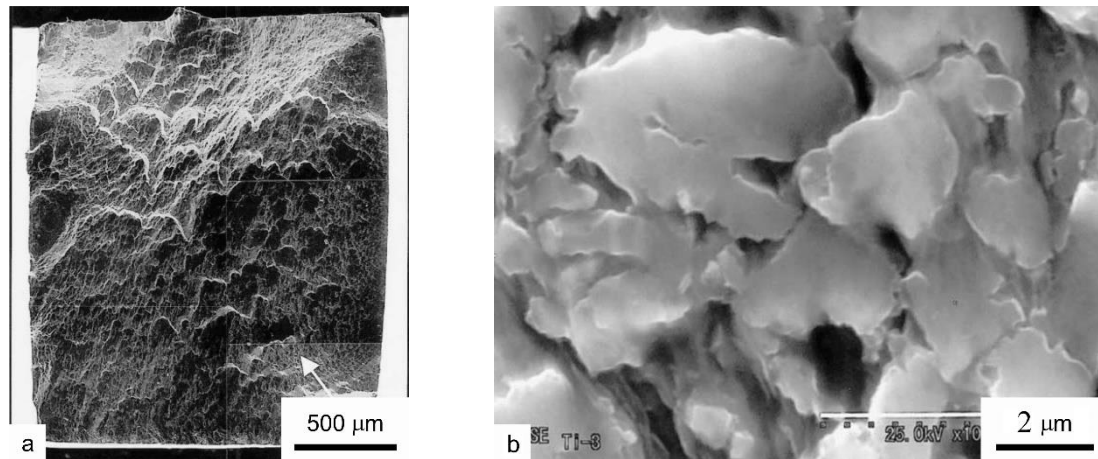


Figure 9. SEM images showing the fracture surface of UFG Ti under constant plastic strain amplitudes: (a) arrow indicates the crack growth direction; (b) the fracture surface morphology reprinted with permission from ref. [31]. Copyright 2001 Elsevier.

The final crack growth occurred predominantly in the plane of the maximum tangential stresses, without macroscopic deflections or branching. The fracture surface of the specimens remained smooth, without any visible stress and damage localization. The crack propagation mechanism was mixed, intercrystalline or transcrystalline, although it was rather difficult to identify due to the local plasticity along the crack path [31]. Thus, in UFG CP Ti, as in other pure metals with an equiaxed UFG structure, the predominance of the intercrystalline fracture mechanism during the fatigue fracture growth was observed experimentally.

This accounts for the almost straight crack path and a relatively smooth fracture surface relief in a homogeneous equiaxed UFG structure, which may be associated with the weakening of grain boundaries captured by lattice dislocations [75].

A somewhat different situation was observed in two-phase Ti alloys. It is known that in conventional Ti alloys, the crack path during cyclic tests is strongly influenced by the morphology of the α -phase: lamellar or bimodal. In particular, according to Nalla et al. [53], in a lamellar structure, the crack path has a more twisted and tortuous character in comparison to, for example, a bimodal microstructure. Correspondingly, the crack propagation rate in a lamellar structure, especially at high stress intensity values, is lower than that in a bimodal structure. That being said, the high-cycle fatigue resistance in a bimodal structure is better than that in a lamellar structure, due to the higher ductility.

Taking into account the high sensitivity to crack growth and microstructural parameters, the crack nucleation and propagation mechanisms in two-phase alloys call for a more careful examination.

Saitova et al. [55] investigated the fracture mechanisms of specimens of Ti-6Al-4V ELI alloy in a UFG state after strain-control tests. It was demonstrated that the fractures had typical fracture surfaces: (I) crack nucleation region, (II) crack propagation region, and (III) rapid fracture region. The distance between striations grew from the crack nucleation site to the crack propagation zone, which indicated an increase in the fatigue crack propagation rate. The main fatigue cracks for all the specimens in the CG and UFG states were predominantly transcrystalline. The character of the secondary microcracks exhibited substantial differences. For example, in the CG alloy, secondary cracks were observed, located at

interphase boundaries or in the β -phase, whereas in the UFG specimens secondary cracks were oriented almost perpendicularly to the main crack. This fact has a beneficial effect on fatigue resistance [55]. According to [59,60], the same character of failure was observed in the UFG Ti-6Al-4V alloy during stress-control tests in the high-cycle and low-cycle fatigue regions. The first cracks nucleated mainly at the surface roughnesses (referred to as slip bands), in grain interiors, and at grain boundaries or interphase boundaries. This was confirmed in [55], showing the surface relief of specimens after cyclic tests with a controlled stress for the CG and UFG states, obtained with an atomic-force microscope. In the surface relief of the specimens, the distribution of the α - and β -phases in the CG and UFG states is clearly distinct. In this case, the common feature of the alloy's surface relief in both states are the visibly distinguishable slip bands in the β -phase, located at a 60° angle to the loading direction.

In a review paper [4], Vinogradov assumes, based on the known research, that the grain refinement and strain hardening limiting the dislocation mobility inevitably result in suppression of the crack tip blunting effect; thus, leading to faster propagation of sharp cracks in the UFG state. In Ti and other pure metals with an equiaxed UFG structure, the intercrystalline fracture mechanism prevails during the growth of a fatigue crack. On the other hand, in Ti alloys, solid-solution strengthening somewhat reduces the effect of grain refinement on the total mechanical response under monotonous and cyclic loads [4]. Here, the role of the second phase, the morphology, and distribution of the secondary phases increases. It can be assumed that alloys with a more complex phase composition will be more susceptible to improvement of the fatigue characteristics during SPD processing. This may be achieved by structural optimization by controlling the secondary phase precipitates, changing the kinetics of their precipitation, and a more uniform distribution in the microstructure. An inhomogeneous structure, e.g., a bimodal one or one with a pronounced crystallographic texture, may lead to a more tortuous crack path and increased crack growth resistance, but this issue remains to be addressed in future research [4].

5. On the Prospects of the Practical Application of Ti-Based Materials in Industry

Ti is known to be the most promising metallic material for medical applications in dentistry, orthopedics, and traumatology [76–78], and the designing of an ultrafine-grained Ti with enhanced properties is the foundation for developing next-generation products. As demonstrated by the research discussed in Section 1, the mechanical properties of CP Ti have been improved to such a degree that it can now replace Ti-6Al-4V alloy, at least in such applications as dental and extraoral (ear) implants. Furthermore, biological experiments with the use of two cell types (human osteosarcoma SaOS-2 cells and adipose-derived mesenchymal stem cells) demonstrated the improved capacity of these cells for attaching, proliferating, and differentiating on the surface of UFG Ti-based materials processed by SPD [79,80]. Insertion of implants made of UFG pure Ti will enable considerably reducing the duration of post-surgery rehabilitation of patients and extend the service life of an inserted implant until its replacement. The advantages of UFG Ti for the production of different types of medical implants are most fully described in the papers and reviews by Elias et al. and Valiev et al. [80–85].

However, the fatigue life data from the tests in a simulated body fluid (SBF) allow one to make contradictory conclusions about the effect of ultrafine grain size [86–88]. The data on the fatigue of Ti implants become even more scattered after a typical surface treatment used in the medical industry [89]. The required microroughness profile on the surface may have a drastic effect on the fatigue life of an implant.

It is known that 'conventional' fatigue test methods, in compliance with ISO standards, involve S/N (stress–number of cycles) curves. However, when applied to an implant structure, they have a significant drawback. This is related to the fact that for a dental implant, the applied loads are practically random. Therefore, the functionality testing of a dental implant is not ensured by standard approaches. Several studies report that in recent years a method was developed for 'random spectrum fatigue performance testing' of dental

implants [90]. It consists in applying a random sequence of loads with different amplitudes and frequencies (and atmospheres), until implant failure. The result for each tested group is the average duration of life with a standard deviation. The developed method of random loading [91,92], used for fatigue tests of implants made of UFG CP Ti in both air and 0.9% saline solution, did not confirm the superior fatigue characteristics of UFG Ti in comparison to coarse-grained CG Ti, as reported in [87].

In [93], an evaluation was made for the advantages of using nanostructured CP Ti for the manufacture of miniature implants for osteosynthesis in the cranio-facial and mandibular areas. The study used Grade 4 Ti rods nanostructured by means of ECAP-C and subsequent drawing. Items in the form of plates and screws with a reduced cross section, but preserving their static and fatigue strength, were designed and produced from nano-Ti. Transverse-bending fatigue tests of the plates were performed using a rigid loading pattern at a constant value of strain amplitude (deflection $f = 3$ mm), loading cycle asymmetry coefficient $R = 0$, and load application frequency of 30 Hz. As a result of the comparative fatigue tests of standard Ti plates and plates made of nanostructured Ti, it was found that a decrease in their cross section does not lead to a considerable decline in their fatigue life. It was shown in [93] that the life (the number of cycles to failure) of a plate made of nanostructured Ti was almost an order higher than the life of the standard item.

At the same time, the application of UFG Ti for the manufacture of medical implants is also associated with the surface modification of products, since they operate in a physiological environment that may have a negative effect on the surface. In particular, it was shown in [94], that the significant grain refinement achieved in Gr2 Ti by means of SPD Conform processing raised the *UTS* by almost two-fold, while the endurance limit increased from 375 MPa to 800 MPa. The surface treatment of implants by sandblasting in combination with acid etching (SLA) reduced the endurance limit of the UFG condition by almost 56%, and by 27% in the case of the CG structure; i.e., the SLA treatment had a larger impairing effect on the fatigue properties of UFG Ti, apparently due to a decreased ductility. This area of research is under active development, and researchers have already proposed methods for the surface modification of implants made of UFG Ti that do not reduce its fatigue strength [95].

Two-phase Ti alloys, due to their high specific strength and corrosion resistance, are widely used in aviation and engine building. Increasing the performance properties of parts and structures made of Ti alloys in conditions of long lifetimes is an important problem in today's mechanical engineering. Therefore, the application of UFG Ti alloys for the manufacture of such critical parts as disks and blades is of great interest, where the critical properties that determine the life and reliability of products are strength, endurance, and wear resistance. In addition, the superplasticity of UFG Ti alloys at low temperatures and higher strain rates, under the condition of the formation of a structure with a grain size below 0.5–1.0 μm [1,2], is technologically attractive, in terms of shape forming, since the traditional process for the production of complex-profile blades from Ti alloys is die forging.

In [96], the authors reported the possibility in principle of producing gas-turbine engine blades from the UFG Ti-6Al-4V titanium alloy. Decreasing the temperature of metal deformation in isothermal forging, not only has processing advantages, but also creates conditions for increasing the service properties of produced articles, due to the preservation of the UFG structure in the alloy. In the study, tests were performed on blades produced using a traditional forging process at 940 °C and blades produced from UFG workpieces by isothermal forging at 720 °C. The tests were performed via the first bending mode of vibration on a special vibration stand with a frequency of 500 Hz, on the basis of 20×10^7 cycles, i.e., in conditions close to the part's operating conditions. The conducted tests confirmed the advantage of the blades with a UFG structure, which exhibited a 30% increase in endurance limit in comparison to the conventional parts. Zherebtsov et al. [42] also reported the possibility of increasing the endurance limit of blades made of Ti-6Al-4V titanium alloy, due to the formation of a SMC structure by multiaxial isothermal forging.

The first reports about the positive effect of a UFG structure on the fatigue endurance of parts made of Ti alloys gave grounds to believe that it would be possible to use them in gas-turbine engines (GTE). However, so far the efforts of researchers have been aimed primarily at increasing the mechanical characteristics of alloys at room temperature. Meanwhile, the formation of a nanostructured state in alloys often leads to a decline in the material's thermal stability at elevated temperatures, due to a high accumulated energy [1]. As a consequence, this strongly limits the practical application of UFG Ti alloys at the operating temperatures of GTE parts. Therefore, a relevant area of further research is the study of the mechanisms and regularities in the evolution of a UFG structure in conditions of a simultaneous exposure to temperature and stresses. In the first place, this includes such performance properties of UFG Ti alloys as creep resistance and fatigue resistance at operating temperature.

Another important aspect for the successful application of Ti alloys with a UFG structure, especially during long-term operation in various aggressive environments, is the interaction of titanium with hydrogen. It is known that hydrogen can easily diffuse from the environment and impair mechanical properties, up to the embrittlement of the near-surface layers. An assumption was made in an overview paper [97] that the formation of a nanostructured state in Ti alloys would enable reducing the effect of H, owing to a considerable increase in the extent of the intergranular boundaries in the microstructure. In this case, the redistribution of the incoming hydrogen occurs via a large number of the crystalline structure defects that are non-equilibrium grain boundaries and deformation defects, which enable avoiding exceeding the limit of solubility of hydrogen in the crystalline lattice. Apparently, the formed hydride particles can be expected to be smaller in size and uniformly distributed in the material volume, predominantly in the intergrain boundaries. From the point of view of hydrogen brittleness, such a state of the hydride phase is less dangerous and enables increasing the value of the maximum permissible H concentration in Ti and its alloys.

This hypothesis was confirmed by several conducted studies [98]. For example, in an NiTi alloy with grain sizes of 23 and 57 μm and with the same times of holding in an APF solution, the sample with the smaller grain size exhibited a lower value of fracture stress and a higher relative fracture strain. Such a behavior makes grain refinement an efficient factor for improving a material's resistance to hydrogen embrittlement, underlain by a decrease in hydrogen's 'effective' diffusion rate value, due to a decrease in the relative fraction of hydrogen per area unit of a grain boundary. Another paper [99] examined the effect of increasing the resistance to hydrogen embrittlement of the UFG Ti-6Al-4V alloy, by means of increasing its maximum permissible hydrogen concentration in comparison to the CG state. A paper [100] showed that the elongation and impact toughness of nanocrystalline Ti with a hydrogen content from 0.1 to 5 at.% are practically the same, while in microcrystalline Ti they decrease when hydrogen is added, which indicates a lower risk of hydride-induced embrittlement in nanocrystalline Ti than in its microcrystalline counterpart. However, this problem calls for targeted studies, especially concerning the fatigue strength of Ti with permissible and increased hydrogen concentrations.

6. Summary

The overview of publications on Ti and the Ti-6Al-4V titanium alloy presented in this paper gives an indication of fatigue resistance in the ultrafine-grained state, based on SPD processing, leading to an increase in the endurance limit (HCF), but reducing or slightly increasing fatigue strength in the low-cycle fatigue (LCF) region. Grain refinement achieved by a set of measures, including SPD processing and subsequent thermomechanical treatment, is very efficient for producing high, even record-breaking, fatigue characteristics in Ti alloys. At the same time, the level of ductility also plays an important role in fatigue resistance. It also becomes obvious that approaches aimed only at increasing the UTS are not always justified, since the fatigue ratio σ_f/σ_{UTS} remains practically unchanged. It was also found that the σ_f/σ_{UTS} ratio for Ti-based materials strengthened by SPD processed

lies in a range from 0.47 to 0.58, i.e., it does not go beyond the limits of the values for conventional annealed and heat-strengthened Ti alloys, which is an important conclusion for future engineering applications of UFG Ti alloys.

Ultrafine-grained Ti demonstrates a tendency, similar to that of many investigated single-phase UFG materials, for the crack propagation rate to increase by the same value as the stress intensity factor range ΔK , which is related to the predominance of the inter-crystalline mechanism of the fatigue crack propagation. In two-phase Ti alloys having an inhomogeneous duplex structure, the transcrystalline character of crack growth prevails, but this requires a more detailed investigation, since, so far, the number of studies on the crack propagation rate in UFG two-phase Ti alloys has been very limited.

The advantages of UFG Ti for the manufacture of different types of medical implants have already been proven and described in many papers and reviews. The first publications on the possibility of using UFG two-phase Ti alloys in GTE were based on the positive effect of a UFG structure on fatigue endurance at room temperature. However, the practical application of UFG Ti alloys in aircraft engine building still requires the detailed investigation of such performance properties as creep resistance and fatigue resistance at an elevated temperature, for long-term strength.

Author Contributions: I.P.S., conceptualization, writing—original draft preparation; Y.M.M., writing—original draft preparation; A.G.S., methodology; A.V.P., writing—review and editing; M.V.P., writing—review and editing. All authors have read and agreed to the published version of the manuscript.

Funding: This work (Sections 2, 4 and 5) was carried out with the financial support of the Ministry of Science and Higher Education of the Russian Federation in the framework of project No. FSNM-2020-0027. Yu. Modina (Section 3) is grateful for the support of activities to the Russian Scientific Foundation, grant №21-79-10167.

Data Availability Statement: Not applicable.

Conflicts of Interest: The authors declare no conflict of interest.

References

1. Valiev, R.Z.; Zhilyaev, A.P.; Langdon, T.G. *Bulk Nanostructured Materials: Fundamentals and Applications*; John Wiley BT & Sons Inc.: Hoboken, NJ, USA, 2013; ISBN 9781118095409.
2. Valiev, R.Z.; Estrin, Y.; Horita, Z.; Langdon, T.G.; Zehetbauer, M.J.; Zhu, Y. Producing Bulk Ultrafine-Grained Materials by Severe Plastic Deformation: Ten Years Later. *JOM* **2016**, *68*, 1216–1226. [[CrossRef](#)]
3. Kapoor, R. Severe Plastic Deformation of Materials. Materials Under Extreme Conditions. In *Materials Under Extreme Conditions. Recent Trends and Future Prospects*; Tyagi, A.K., Banerjee, S., Eds.; Elsevier: Amsterdam, The Netherlands, 2017; pp. 717–754. [[CrossRef](#)]
4. Estrin, Y.; Vinogradov, A. Fatigue behaviour of light alloys with ultrafine grain structure produced by severe plastic deformation: An overview. *Int. J. Fatigue* **2010**, *32*, 898–907. [[CrossRef](#)]
5. Terent'ev, V.F. *Fatigue Strength of Metals and Alloys*; Intermet Engineering: Moscow, Russia, 2002; p. 288.
6. Hanlon, T.; Tabachnikova, E.; Suresh, S. Fatigue behavior of nanocrystalline metals and alloys. *Int. J. Fatigue* **2005**, *27*, 1147–1158. [[CrossRef](#)]
7. Vinogradov, A.; Hashimoto, S. Multiscale Phenomena in Fatigue of Ultra-Fine Grain Materials-an Overview. *Mater. Trans.* **2001**, *42*, 74–84. [[CrossRef](#)]
8. Agnew, S.R.; Vinogradov, A.Y.; Hashimoto, S.; Weertman, J.R. Overview of fatigue performance of Cu processed by severe plastic deformation. *J. Electron. Mater.* **1999**, *28*, 1038–1044. [[CrossRef](#)]
9. Mughrabi, H.; Höppel, H.W. Cyclic Deformation and Fatigue Properties of Ultrafine Grain Size Materials: Current Status and Some Criteria for Improvement of the Fatigue Resistance. *Mater. Res. Soc. Symp. Proc.* **2000**, *634*, B2.1.1–B2.1.12. [[CrossRef](#)]
10. Maier, H.; Gabor, P.; Gupta, N.; Karaman, I.; Haouaoui, M. Cyclic stress–strain response of ultrafine grained copper. *Int. J. Fatigue* **2006**, *28*, 243–250. [[CrossRef](#)]
11. Dalla-Torre, F.; Lapovok, R.; Sandlin, J.; Thomson, P.F.; Davies, C.H.J.; Pereloma, E.V. Microstructures and properties of copper processed by equal channel angular extrusion for 1–16 passes. *Acta Mater.* **2004**, *52*, 4819–4832. [[CrossRef](#)]
12. Höppel, H.W.; Mughrabi, H.; Vinogradov, A. Fatigue Properties of Bulk Nanostructured Materials. In *Bulk Nanostructured Materials*, 1st ed.; Zehetbauer, M.J., Zhu, Y.T., Eds.; Wiley-VCH: Weinheim, Germany, 2009; pp. 481–500. [[CrossRef](#)]
13. Vinogradov, A. Fatigue limit and crack growth in ultra-fine grain metals produced by severe plastic deformation. *J. Mater. Sci.* **2006**, *42*, 1797–1808. [[CrossRef](#)]

14. Vinogradov, A.Y.; Agnew, S.R. Nanocrystalline Materials: Fatigue. In *Dekker Encyclopedia of Nanoscience and Nanotechnology*, 3rd ed.; Lyshevski, S.E., Ed.; Taylor & Francis Group LLC: Abingdon, UK, 2005; pp. 1–20.
15. Vinogradov, A.; Nagasaki, S.; Patlan, V.; Kitagawa, K.; Kawazoe, M. Fatigue properties of 5056 Al-Mg alloy produced by equal-channel angular pressing. *Nanostruct. Mater.* **1999**, *11*, 925–934. [[CrossRef](#)]
16. Chung, C.S.; Kim, J.K.; Kim, H.K.; Kim, W.J. Improvement of high-cycle fatigue life in a 6061 Al alloy produced by equal channel angular pressing. *Mater. Sci. Eng. A* **2002**, *337*, 39–44. [[CrossRef](#)]
17. Höppel, H.W.; Valiev, R.Z. On the possibilities to enhance the fatigue properties of ultrafine-grained metals. *Z. Met.* **2002**, *93*, 641–648.
18. Turner, N.G.; Roberts, W.T. Fatigue behavior of titanium. *Trans. AIME* **1968**, *242*, 1223–1230.
19. Sugano, M.; Kanno, S.; Satake, T. Fatigue behaviour of titanium in vacuum. *Acta Metall.* **1989**, *37*, 1811–1820. [[CrossRef](#)]
20. Tokaji, K.; Ogawa, T.; Ohya, K. The effect of grain size on small fatigue crack growth in pure titanium. *Int. J. Fatigue* **1994**, *16*, 571–578. [[CrossRef](#)]
21. Takao, K.; Kusakawa, K. Low-cycle fatigue behavior of commercially pure titanium. *Mater. Sci. Eng. A* **1996**, *213*, 81–85. [[CrossRef](#)]
22. Gerberich, W.W.; Harvey, S.E.; Kramer, D.E.; Hoehn, J.W. Low and high cycle fatigue—A continuum supported by AFM observations. *Acta Mater.* **1998**, *46*, 5007–5021. [[CrossRef](#)]
23. Sugano, M.; Tanaka, N.; Sakuma, E.; Satake, T. *Proceedings of the 8th World Congress on Titanium (Titanium '95)*, Birmingham, UK, 22–26 October 1995; Institute of Materials: London, UK, 1996; p. 1131.
24. Suresh, S. *Fatigue of Materials*, 2nd ed.; Cambridge University Press: Cambridge, UK, 1998; p. 617.
25. Zharebtsov, S.; Semenova, I.P.; Halina, G.; Motyka, M. Advanced Mechanical Properties. In *Nanocrystalline Titanium*; Garbacz, H., Semenova, I., Eds.; Zharebtsov Sergey Maciej Motyka Elsevier Inc.: Amsterdam, The Netherlands, 2019; pp. 103–121.
26. Zharebtsov, S.V. Strength and ductility-related properties of ultrafine grained two-phase titanium alloy produced by warm multiaxial forging. *Mater. Sci. Eng. A* **2012**, *536*, 190–196. [[CrossRef](#)]
27. Semenova, I.P.; Raab, G.I.; Valiev, R.Z. Nanostructured Titanium Alloys: New Developments and Application Prospects. *Nanotechnol. Russ.* **2014**, *9*, 320–333. [[CrossRef](#)]
28. Semenova, I.P.; Polyakova, V.V.; Dyakonov, G.S.; Polyakov, A.V. Ultrafine-Grained Titanium-Based Alloys: Structure and Service Properties for Engineering Applications. *Adv. Eng. Mater.* **2019**, *22*, 1900651. [[CrossRef](#)]
29. Stolyarov, V.V.; Latysh, V.V.; Valiev, R.Z.; Zhu, Y.T.; Lowe, T.C.; Valiev, R.Z. (Eds.) *Investigations and Applications of Severe Plastic Deformation*; NATO Science Series, v.3/80; Kluwer Publishers: Dordrecht, The Netherlands, 2000; p. 367.
30. Stolyarov, V.V.; Alexandrov, I.V.; Kolobov, Y.R.; Zhu, M.; Zhu, Y.; Lowe, T. *Proceedings of the Seventh International Fatigue Congress, Beijing, China, 8–12 June 1999*; Wu, X.R., Wang, Z.G., Eds.; Higher Education Press: Beijing, China, 1999; p. 1345.
31. Vinogradov, A.Y.; Stolyarov, V.V.; Hashimoto, S.; Valiev, R.Z. Cyclic behavior of ultrafine-grain titanium produced by severe plastic deformation. *Mater. Sci. Eng. A* **2001**, *318*, 163–173. [[CrossRef](#)]
32. Vinogradov, A.; Hashimoto, S. Fatigue of Severely Deformed Materials. In *Nanomaterials by Severe Plastic Deformation*; Zehetbauer, M.J., Valiev, R.Z., Eds.; Wiley-VCH: Weinheim, Germany, 2004; pp. 663–676.
33. Wang, K. The use of titanium for medical applications in the USA. *Mater. Sci. Eng. A* **1996**, *213*, 134–137. [[CrossRef](#)]
34. Agnew, S.; Weertman, J. Cyclic softening of ultrafine grain copper. *Mater. Sci. Eng. A* **1998**, *244*, 145–153. [[CrossRef](#)]
35. Hoppel, H.W.; Brunnbauer, M.; Mughrabi, H.; Valiev, R.Z.; Zhilyaev, A. *Proceedings of the International Congress on Advanced Materials, Processes and Applications, Munich, Germany, 25–28 September 2000, Munich Materials Week 2000*; Werkstoffwoche-Partnerschaft GbR: Frankfurt, Germany, 2000.
36. Semenova, I.P.; Salimgareeva, G.K.; Latysh, V.V.; Kunavin, S.A.; Valiev, R.Z. Fatigue resistance of titanium with ultrafine-grained structure. *Met. Sci. Heat. Treat.* **2009**, *51*, 87–91. [[CrossRef](#)]
37. Boyer, R.; Welsch, G.; Collings, E.W. (Eds.) *Materials Properties Handbook: Titanium Alloys*; ASM International: Novelty, OH, USA, 1998.
38. Semenova, I.P.; Salimgareeva, G.H.; Costa, G.D.; Lefebvre, W.; Valiev, R.Z. Enhanced strength and ductility of ultra-fine grained Ti processed by severe plastic deformation. *Adv. Eng. Mater.* **2010**, *12*, 803–807. [[CrossRef](#)]
39. Semenova, I.P.; Valiev, R.Z.; Yakushina, E.B.; Salimgareeva, G.H.; Lowe, T.C. Strength and fatigue properties enhancement in ultrafine-grained Ti produced by severe plastic deformation. *J. Mater. Sci.* **2008**, *43*, 7354–7359. [[CrossRef](#)]
40. Semenova, I.P.; Yakushina, E.B.; Nurgaleeva, V.V.; Valiev, R.Z. Nanostructuring of Ti-alloys by SPD processing to achieve superior fatigue properties. *Int. J. Mater. Res.* **2009**, *100*, 1691–1696. [[CrossRef](#)]
41. Semenova, I.P.; Polyakov, A.V.; Raab, G.I.; Lowe, T.C.; Valiev, R.Z. Enhanced fatigue properties of ultrafine-grained Ti rods processed by ECAP-Conform. *J. Mater. Sci.* **2012**, *47*, 7777–7781. [[CrossRef](#)]
42. Zharebtsov, S.; Salishchev, G. Production, Properties and Application of Ultrafine-Grained Titanium Alloys. *Mater. Sci. Forum* **2016**, *838–839*, 294–301. [[CrossRef](#)]
43. Garbacz, H.; Pakiela, Z.; Kurzydowski, K.J. Fatigue properties of nanocrystalline titanium. *Rev. Adv. Mater. Sci.* **2010**, *25*, 256–260.
44. Lanning, D.; Haritos, G.K.; Nicholas, T.; Maxwell, D.C. Low-cycle fatigue/high-cycle fatigue interactions in notched Ti-6Al-4V*. *Fatigue Fract. Eng. Mater. Struct.* **2001**, *24*, 565–577. [[CrossRef](#)]
45. Kim, W.-J.; Hyun, C.-Y.; Kim, H.-K. Fatigue strength of ultrafine-grained pure Ti after severe plastic deformation. *Scr. Mater.* **2006**, *54*, 1745–1750. [[CrossRef](#)]

46. Semenova, I.P.; Salimgareeva, G.K.; Latysh, V.V.; Lowe, T.; Valiev, R.Z. Enhanced fatigue strength of commercially pure Ti processed by severe plastic deformation. *Mater. Sci. Eng. A* **2009**, *503*, 92–95. [[CrossRef](#)]
47. Liu, X.; Chu, P.; Ding, C. Surface modification of titanium, titanium alloys, and related materials for biomedical applications. *Mater. Sci. Eng. R Rep.* **2004**, *47*, 49–121. [[CrossRef](#)]
48. Polyakov, A.V.; Raab, G.I.; Semenova, I.P.; Valiev, R.Z. Mechanical properties of UFG titanium: Notched fatigue and impact toughness. *Mater. Lett.* **2021**, *302*, 130366. [[CrossRef](#)]
49. Baek, S.M.; Polyakov, A.V.; Moon, J.H.; Semenova, I.P.; Valiev, R.Z.; Kim, H.S. Effect of surface etching on the tensile behavior of coarse- and ultrafine-grained pure titanium. *Mater. Sci. Eng. A* **2017**, *707*, 337–343. [[CrossRef](#)]
50. Lutjering, G.; Williams, J.C. *Titanium*; Springer: Berlin/Heidelberg, Germany; New York, NY, USA, 2007.
51. Veiga, C.; Davim, J.P.; Loureiro, A.J.R. Properties and applications of titanium alloys: A brief review. *Rev. Adv. Mater. Sci.* **2012**, *32*, 133–148.
52. Peters, M.; Hemptenmacher, J.; Kumpfert, J.; Leyens, C. Structure and Properties of Titanium and Titanium Alloys. In *Titanium and Titanium Alloys, Fundamentals and Applications*; Leyens, C., Peters, M., Eds.; Wiley-VCH: Weinheim, Germany, 2005; pp. 1–36. [[CrossRef](#)]
53. Nalla, R.K.; Ritchie, R.O.; Boyce, B.L.; Campbell, J.P.; Peters, J.O. Influence of microstructure on high-cycle fatigue of Ti-6Al-4V: Bimodal vs. lamellar structures. *Metall. Mater. Trans. A* **2002**, *33*, 899–918. [[CrossRef](#)]
54. Zhrebtsov, S.; Salishchev, G.; Galeev, R.; Maekawa, K. Mechanical Properties of Ti-6Al-4V Titanium Alloy with Submicrocrystalline Structure Produced by Severe Plastic Deformation. *Mater. Trans.* **2005**, *46*, 2020–2025. [[CrossRef](#)]
55. Saitova, L.R.; Höppel, H.W.; Göken, M.; Semenova, I.P.; Raab, G.I.; Valiev, R.Z. Fatigue behavior of ultrafine-grained Ti-6Al-4V “ELI” alloy for medical applications. *Mater. Sci. Eng. A* **2009**, *503*, 145–147. [[CrossRef](#)]
56. Saitova, L.; Hoppel, H.; Goken, M.; Semenova, I.; Valiev, R. Cyclic deformation behavior and fatigue lives of ultrafine-grained Ti-6Al-4V ELI alloy for medical use. *Int. J. Fatigue* **2009**, *31*, 322–331. [[CrossRef](#)]
57. Zhrebtsov, S.V. Efficiency of the strengthening of titanium and titanium alloys of various classes by the formation of an ultrafine-grained structure via severe plastic deformation. *Russ. Metall. (Metally)* **2012**, *2012*, 969–974. [[CrossRef](#)]
58. Zhrebtsov, S.V.; Kostjuchenko, S.; Kudryavtsev, E.A.; Malysheva, S.; Murzinova, M.A.; Salishchev, G.A. Mechanical Properties of Ultrafine Grained Two-Phase Titanium Alloy Produced by “abc” Deformation. *Mater. Sci. Forum* **2012**, *706–709*, 1859–1863. [[CrossRef](#)]
59. Polyakov, A.V.; Semenova, I.P.; Huang, Y.; Valiev, R.Z.; Langdon, T.G. Fatigue Life and Failure Characteristics of an Ultrafine-Grained Ti-6Al-4V Alloy Processed by ECAP and Extrusion. *Adv. Eng. Mater.* **2014**, *16*, 1038–1043. [[CrossRef](#)]
60. Semenova, I.P.; Polyakov, A.V.; Polyakova, V.V.; Huang, Y.; Valiev, R.Z.; Langdon, T.G. High-Cycle Fatigue Behavior of an Ultrafine-Grained Ti-6Al-4V Alloy Processed by ECAP and Extrusion. *Adv. Eng. Mater.* **2016**, *18*, 2057–2062. [[CrossRef](#)]
61. Hoppel, H.; Kautz, M.; Xu, C.; Murashkin, M.; Langdon, T.; Valiev, R.; Mughrabi, H. An overview: Fatigue behaviour of ultrafine-grained metals and alloys. *Int. J. Fatigue* **2006**, *28*, 1001–1010. [[CrossRef](#)]
62. Salishchev, G.A.; Galeev, R.M.; Malysheva, S.P.; Zhrebtsov, S.V.; Mironov, S.Y.; Valiakhmetov, O.R.; Ivanisenko, É.I. Formation of submicrocrystalline structure in titanium and titanium alloys and their mechanical properties. *Met. Sci. Heat Treat.* **2006**, *48*, 63–69. [[CrossRef](#)]
63. Hübner, P.; Kiessling, R.; Biermann, H.; Hinkel, T.; Jungnickel, W.; Kawalla, R.; Höppel, H.W.; May, J. Static and Cyclic Crack Growth Behavior of Ultrafine-Grained Al Produced by Different Severe Plastic Deformation Methods. *Metall. Mater. Trans. A* **2007**, *38*, 1926–1933. [[CrossRef](#)]
64. Meyers, L.W.; Sommer, K.; Halle, T.; Hockauf, M. Crack growth in ultrafine-grained AA6063 produced by equal-channel angular pressing. *J. Mater. Sci.* **2008**, *43*, 7426–7431. [[CrossRef](#)]
65. Hübner, P.; Kiessling, R.; Biermann, H.; Vinogradov, A. Fracture behaviour of ultrafine-grained materials under static and cyclic loading. *Int. J. Mater. Res.* **2006**, *97*, 1566–1570. [[CrossRef](#)]
66. Pao, P.; Jones, H.; Cheng, S.; Feng, C. Fatigue crack propagation in ultrafine grained Al-Mg alloy. *Int. J. Fatigue* **2005**, *27*, 1164–1169. [[CrossRef](#)]
67. Cavaliere, P. Fatigue properties and crack behavior of ultra-fine and nanocrystalline pure metals. *Int. J. Fatigue* **2009**, *31*, 1476–1489. [[CrossRef](#)]
68. Collini, L. Fatigue crack growth resistance of ECAPed ultrafine-grained copper. *Eng. Fract. Mech.* **2010**, *77*, 1001–1011. [[CrossRef](#)]
69. Meyer, L.W.; Sommer, K.; Halle, T.; Hockauf, M. Microstructure and Mechanical Properties Affecting Crack Growth Behaviour in AA6060 Produced by Equal-Channel Angular Extrusion. *Mater. Sci. Forum.* **2008**, *584–586*, 815–820. [[CrossRef](#)]
70. Tang, G.C.H. Fatigue Crack Growth of Ultra Fine Grained Aluminium. Ph.D. Thesis, School of Materials Science & Engineering, University of New South Wales, Kensington, Australia, 2012.
71. Pugno, N.; Ciavarella, M.; Cornetti, P.; Carpinteri, A. A generalized Paris’ law for fatigue crack growth. *J. Mech. Phys. Solids* **2006**, *54*, 1333–1349. [[CrossRef](#)]
72. Klevtsov, G.V.; Valiev, R.Z.; Botvina, L.R.; Klevtsova, N.A.; Semenova, I.P.; Kashapov, M.R.; Fesenyuk, M.V.; Soldatenkov, A.P. Kinetics of the fatigue failure of Ti in a submicrocrystalline state. *Vestn. Orenbg. State Univ.* **2012**, *9*, 123–125. (In Russian)
73. Yarema, S.Y. Assessment of metal and alloy resistance to cracking. studies of fatigue crack growth and kinetic fatigue fracture diagrams. *Sov. Mater. Sci.* **1978**, *13*, 351–368. [[CrossRef](#)]

74. Klevtsov, G.V.; Valiev, R.Z.; Semenova, I.P.; Klevtsova, N.A.; Danilov, V.A.; Linderov, M.L.; Zasytkin, S.V. Influence of Ultrafine-Grained Structure on the Kinetics and Fatigue Failure Mechanism of VT6 Titanium Alloy. *Russ. J. Non-Ferr. Met.* **2019**, *60*, 253–258. [[CrossRef](#)]
75. Thompson, A.W.; Backofen, W.A. The effect of grain size on fatigue. *Acta Metall.* **1971**, *19*, 597–606. [[CrossRef](#)]
76. Rodríguez-Mercado, J. Genotoxic effects of vanadium(IV) in human peripheral blood cells. *Toxicol. Lett.* **2003**, *144*, 359–369. [[CrossRef](#)]
77. Bondy, S.C. The neurotoxicity of environmental aluminum is still an issue. *Neurotoxicology* **2010**, *31*, 575–581. [[CrossRef](#)] [[PubMed](#)]
78. Williams, D.F. Titanium for Medical Applications. In *Titanium in Medicine*; Brunette, D., Tengvall, P., Textor, M., Thomson, P., Eds.; Springer: Berlin/Heidelberg, Germany, 2001; pp. 14–24.
79. Estrin, Y.; Lapovok, R.; Medvedev, A.E.; Kasper, C.; Ivanova, E.; Lowe, T.C. Mechanical Performance and Cell Response of Pure Titanium with Ultrafine-Grained Structure Produced by Severe Plastic Deformation. In *Titanium in Medical and Dental Applications*, 1st ed.; Froes, F., Qian, M., Eds.; Woodhead Publishing: Cambridge, UK, 2018; pp. 419–454. [[CrossRef](#)]
80. Medvedev, A.E.; Neumann, A.; Ng, H.P.; Lapovok, R.; Kasper, C.; Lowe, T.C.; Anumalasetty, V.N.; Estrin, Y. Combined effect of grain refinement and surface modification of pure titanium on the attachment of mesenchymal stem cells and osteoblast-like SaOS-2 cells. *Mater. Sci. Eng. C* **2017**, *71*, 483–497. [[CrossRef](#)] [[PubMed](#)]
81. Elias, C.N.; Meyers, M.A.; Valiev, R.Z.; Monteiro, S.N. Ultrafine grained titanium for biomedical applications: An overview of performance. *J. Mater. Res. Technol.* **2013**, *2*, 340–350. [[CrossRef](#)]
82. Polyakov, A.V.; Dyakonov, G.S.; Semenova, I.P.; Raab, G.I.; Dluhos, L.; Valiev, R.Z. Development and study of medical implants made from nanostructured titanium. *Adv. Biomater. Dev. Med.* **2015**, *2*, 63–69.
83. Valiev, R.Z.; Semenova, I.P.; Latysh, V.V.; Rack, H.; Lowe, T.C.; Petruzalka, J.; Dluhos, L.; Hrusak, D.; Sochova, J. Nanostructured Titanium for Biomedical Applications. *Adv. Eng. Mater.* **2008**, *10*, B15–B17. [[CrossRef](#)]
84. Klevtsov, G.V.; Valiev, R.Z.; Klevtsova, N.A.; Alexandrov, I.V.; Matchin, A.A.; Tyurkov, M.N.; Fesenyuk, M.V. Strength and fracture mechanism of nanomaterials and medical products. *Mater. Tech. Des.* **2021**, *3*, 42–45. [[CrossRef](#)]
85. Elias, C.N.; Fernandes, D.J.; Galiza, J.A.; dos Santos Monteiro, E.; de Almeida, A.C.C. Dental Application. Ch. 12. In *Nanocrystalline Titanium*; Garbacz, H., Semenova, I.P., Zherebtsov, S., Motyka, M., Eds.; Elsevier: Amsterdam, The Netherlands, 2019; pp. 237–253. [[CrossRef](#)]
86. Estrin, Y.; Ivanova, E.P.; Michalska, A.; Truong, V.K.; Lapovok, R.; Boyd, R. Accelerated stem cell attachment to ultrafine grained titanium. *Acta Biomater* **2011**, *7*, 900–906. [[CrossRef](#)]
87. Medvedev, A.E.; Lapovok, R.; Estrin, Y.; Lowe, T.C.; Anumalasetty, V.N. Bending Fatigue Testing of Commercial Purity Titanium for Dental Implants. *Adv. Eng. Mater.* **2016**, *18*, 1166–1173. [[CrossRef](#)]
88. Medvedev, A.E.; Ng, H.P.; Lapovok, R.; Estrin, Y.; Lowe, T.C.; Anumalasetty, V.N. Effect of bulk microstructure of commercially pure titanium on surface characteristics and fatigue properties after surface modification by sand blasting and acid-etching. *J. Mech. Behav. Biomed. Mater.* **2016**, *57*, 55–68. [[CrossRef](#)]
89. Conforto, E.; Aronsson, B.-O.; Salito, A.; Crestou, C.; Caillard, D. Rough surfaces of titanium and titanium alloys for implants and prostheses. *Mater. Sci. Eng. C* **2004**, *24*, 611–618. [[CrossRef](#)]
90. Shemtov-Yona, K.; Rittel, D. Random spectrum loading of dental implants: An alternative approach to functional performance assessment. *J. Mech. Behav. Biomed. Mater.* **2016**, *62*, 1–9. [[CrossRef](#)]
91. Shemtov-Yona, K.; Rittel, D. Fatigue failure of dental implants in simulated intraoral media. *J. Mech. Behav. Biomed. Mater.* **2016**, *62*, 636–644. [[CrossRef](#)]
92. Rittel, D.; Shemtov-Yona, K.; Lapovok, R. Random spectrum fatigue performance of severely plastically deformed titanium for implant dentistry applications. *J. Mech. Behav. Biomed. Mater.* **2018**, *83*, 94–101. [[CrossRef](#)]
93. Semenova, I.P.; Klevtsov, G.V.; Klevtsova, N.A.; Dyakonov, G.S.; Matchin, A.A.; Valiev, R.Z. Nanostructured Titanium for Maxillofacial Mini-Implants. *Adv. Eng. Mater.* **2016**, *18*, 1216–1224. [[CrossRef](#)]
94. Fintova, S.; Dlhý, P.; Mertova, K.; Chlup, Z.; Duchek, M.; Prochazka, R.; Hutar, P. Fatigue properties of UFG Ti grade 2 dental implant vs. conventionally tested smooth specimens. *J. Mech. Behav. Biomed. Mater.* **2021**, *123*, 104715. [[CrossRef](#)]
95. Guo, T.; Gulati, K.; Arora, H.; Han, P.; Fournier, B.; Ivanovski, S. Orchestrating soft tissue integration at the transmucosal region of titanium implants. *Acta Biomater.* **2021**, *124*, 33–49. [[CrossRef](#)]
96. Semenova, I.P.; Raab, G.I.; Polyakova, V.V.; Izmailova, N.F.; Pavlinich, S.P.; Valiev, R.Z. Ultrafine-grained Ti-6Al-4V-alloy used for production of complex-shaped articles with enhanced service properties. *Rev. Adv. Mater. Sci.* **2012**, *31*, 179–184.
97. Kolobov, Y.R. Nanotechnologies for the formation of medical implants based on titanium alloys with bioactive coatings. *Nanotechnol. Russ.* **2009**, *4*, 758–775. [[CrossRef](#)]
98. Asadipour, H.; Doostmohammadi, A.; Saeidi, N.; Moshref-Javadi, M. Effect of Microstructure on Hydrogen Embrittlement and Mechanical Properties of NiTi Biomaterials. *Phys. Met. Metallogr.* **2019**, *120*, 740–749. [[CrossRef](#)]
99. Naydenkin, E.V.; Ratochka, I.V.; Grabovetskaya, G.P. The Aspects of Practical Application of Ultrafine-Grained Titanium Alloys Produced by Severe Plastic Deformation. *Mater. Sci. Forum.* **2010**, *667–669*, 1183–1187. [[CrossRef](#)]
100. Murzinova, M.A.; Salishchev, G.A. Effect of Decrease of Hydride-Induced Embrittlement in Nanocrystalline Titanium. *Adv. Eng. Mater.* **2010**, *12*, 765–768. [[CrossRef](#)]